this behavior of the cobalt(II) center is not revealed by these studies, but would require complete thermodynamic data on these systems. The order of complexing ability for the bases reported is certainly an unusual one.

**Acknowledgment.** The authors acknowledge the support of this research by the National Science Foundation.

**Supplementary Material Available:** a tabulation of all chemical shift data of *N*-MeIm and Co(SMDPT) (Table A) and *N*-MeIm and Ni(SMDPT) (Table B) (5 pages). Ordering information is given on any current masthead page.

## References and Notes

(1) B. S. Tovrog and R. S. Drago, *J. Am. Chem. Soc.*, **96**, 2743 (1974).
(2) D. Doonan and A. L. Balch, *J. Am. Chem. Soc.*, **97**, 1403 (1975). These authors complained with good reason that "experimental conditions were not described with sufficient precision in our earlier report to enable one to determine if the observed shifts were the result of dilution or complexation. No attempt was made to correspond and obtain this information, and the authors incorrectly concluded that our results in Figures 3 and 4 were carried out in $CH_2Cl_2$ instead of $CHCl_3$. We agree that the ambiguities discussed by Doonan and Balch exist in our earlier system and sought a more straightforward system for demonstrating the ambidentate nature of the imidazole ring system.
(3) L. Sacconi and I. Bertini, *J. Am. Chem. Soc.*, **88**, 5180 (1966).
(4) (a) P. L. Orioli, M. DiVaira, and L. Sacconi, *Chem. Commun.*, 300 (1966); (b) M. DiVaira, P. L. Orioli, and L. Sacconi, *Inorg. Chem.*, **10**, 553 (1971).
(5) G. N. LaMar and L. Sacconi, *J. Am. Chem. Soc.*, **89**, 2282 (1967).
(6) I. Bertini, L. Sacconi, and G. P. Speroni, *Inorg. Chem.*, **11**, 1323 (1972).
(7) Observed line widths in **1** are larger than those in **2** due to longer $\tau_e$. It is not known if the "doubling" is obscured at higher temperatures because of the larger line widths or if a rapid exchange between different geometries is slowed at low temperatures.
(8) W. D. Perry and R. S. Drago, *J. Am. Chem. Soc.*, **93**, 2183 (1971).
(9) For a tabulation of all chemical shift data upon coordination to *N*-MeIm, see microfilm edition.
(10) R.-M. Claramunt, J. Elguero, and R. Jacquier, *Org. Magn. Reson.*, **3**, 595 (1971).
(11) R. Cramer and R. S. Drago, *J. Am. Chem. Soc.* **92**, 66 (1970).
(12) D. Doddrell and J. D. Roberts, *J. Am. Chem. Soc.*, **92**, 6839 (1970).
(13) W. DeW. Horrocks and D. L. Johnston, *Inorg. Chem.*, **10**, 1835 (1971).
(14) M. Wicholas, R. Mustacich, B. Johnson, T. Smedley, and J. May, *J. Am. Chem. Soc.*, **97**, 2113 (1975).
(15) R. G. Sievers, Ed., "Nuclear Magnetic Resonance Shift Reagents", Academic Press, New York, N.Y., 1973.
(16) I. Bertini and D. Gatteschi, *Inorg. Chem.*, **12**, 2740 (1973).
(17) R. J. Fitzgerald and R. S. Drago, *J. Am. Chem. Soc.*, **90**, 2523 (1968).
(18) R. J. Fitzgerald and R. S. Drago, *J. Am. Chem. Soc.*, **89**, 2879 (1967).
(19) See T. J. Swift in "NMR of Paramagnetic Molecules", W. DeW. Horrocks, Jr., and G. N. LaMar, Ed., Academic Press, New York, N.Y., 1973.
(20) See C. Langford and T. S. Stengle in ref 19.
(21) W. R. Scheidt, *J. Am. Chem. Soc.*, **96**, 90 (1974).

# On the Photochemical Substitution Reactions of Hexacoordinated Transition Metal Complexes

**L. G. Vanquickenborne* and A. Ceulemans**

*Contribution from the Department of Chemistry, University of Leuven, Celestijnenlaan 200F, B-3030 Heverlee, Belgium.* *Received April 12, 1976*

**Abstract:** The two empirical rules of Adamson were the first attempt to provide a qualitative description of the photochemical substitution reactions of transition metal compounds. It is our purpose (i) to offer an alternative to Adamson's rules (ii) to rationalize the photochemistry by means of a simple model. The model is based on a ligand field approach where the contribution of each ligand is additive in the orbital energy. In a $D_{4h}$ environment, this contribution depends on whether the ligand is in axial or equatorial position. In order to account for the bonding interactions, it is assumed that the ligand basis orbitals are stabilized to the same extent that the metal orbitals are destabilized. Energy expressions have been derived for $d^3$ and $d^6$ systems, in each case for $\sigma$-donor, $\pi$-donor, and $\pi$-acceptor ligands. Using the strong field wave functions, the relevant bond energies in the photoactive states can be calculated. Comparison with the available experimental data on Cr(III) and Co(III) complexes yields a very satisfactory agreement between theory and experiment.

Irradiation of transition metal complexes in the ligand field part of their spectrum gives rise to a strongly enhanced substitution activity. It is well known that the photoexcitation induces the exchange of ligands from the primary coordination sphere with solvent molecules, or with free ligands from the solution.[1,2]

Most of these photochemical substitution reactions of octahedral complexes seem to be governed by two rules, first formulated by Adamson:[3] (i) the leaving ligand is situated on the axis characterized by the weakest ligand field; (ii) of the two ligands situated on the labilized axis, the leaving ligand is the one exhibiting the strongest ligand field.

It is the purpose of this note to formalize in a very simple way the chemical intuition behind Adamson's empirical rules. With this object in view, a number of theoretical models have already been introduced and the groundwork has been laid for understanding ligand field photochemistry.[4-11,28] Although the present approach will be utterly unsophisticated, it goes beyond the existing models in its way of predicting the labilized ligand without needing extensive molecular orbital calculations.

## Description of the Model

Consider a metal ion in an octahedral environment with the six ligands on the three coordinate axes. Consider a one-electron problem, with a metal basis set consisting of the five d orbitals. Within the framework of an additive angular overlap model, one has to specify two parameters, $\sigma_L$ and $\pi_L$, for each ligand L.[12-14] The relevant perturbation matrix is shown in eq 1. While the general complex with six different ligands has no symmetry whatsoever, the matrix is seen to correspond to at least $D_{2h}$ symmetry. Indeed, the parameters always appear as sums of pairs on the same axis, for instance $\sigma_z + \sigma_{-z}$, $\pi_y + \pi_{-y}$, etc. These sums can obviously be replaced by $2\bar{\sigma}_z = (\sigma_z + \sigma_{-z})$, $2\bar{\pi}_y = (\pi_y + \pi_{-y})$, etc., so that one is left with six effective, average parameters, one $(\bar{\sigma}, \bar{\pi})$ set for each axis. If the perturbation along the three axes is equal, the effective (holoheder) symmetry is $O_h$; if two axes ($x$ and $y$) are perturbed in the same way, but different from the third one ($z$), the effective symmetry is $D_{4h}$; if they are all different, the holoheder symmetry[15] is still at least $D_{2h}$. In the latter case,

| | $z^2$ | $yz$ | $xz$ | $xy$ | $x^2-y^2$ |
|---|---|---|---|---|---|
| $z^2$ | $\sigma_z + \sigma_{-z} + {}^1/_4(\sigma_x + \sigma_{-x} + \sigma_y + \sigma_{-y})$ | | | | $-\frac{\sqrt{3}}{4}(\sigma_x + \sigma_{-x} - \sigma_y - \sigma_{-y})$ |
| $yz$ | | $\pi_z + \pi_{-z} + \pi_y + \pi_{-y}$ | | | |
| $xz$ | | | $\pi_z + \pi_{-z} + \pi_x + \pi_{-x}$ | | |
| $xy$ | | | | $\pi_x + \pi_{-x} + \pi_y + \pi_{-y}$ | |
| $x^2-y^2$ | $-\frac{\sqrt{3}}{4}(\sigma_x + \sigma_{-x} - \sigma_y - \sigma_{-y})$ | | | | ${}^3/_4(\sigma_x + \sigma_{-x} + \sigma_y + \sigma_{-y})$ |

(1)

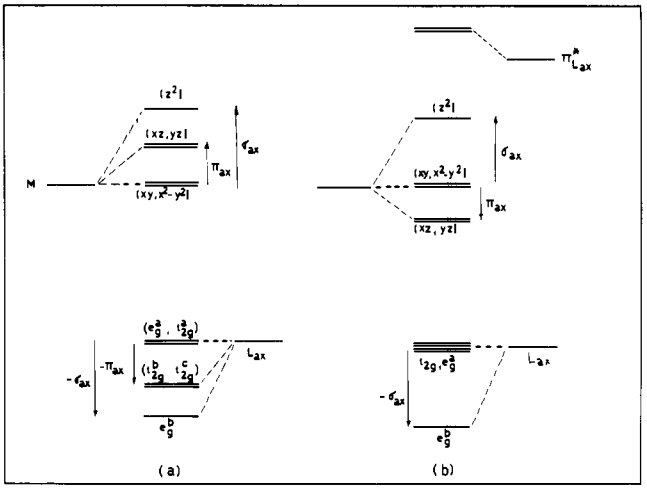


**Figure 1.** Schematic energy level diagram for the interaction of a metal $d^1$ system and one axial ligand: (a) $L_{ax}$ is a $\pi$-donor, (b) $L_{ax}$ is a $\pi$-acceptor.

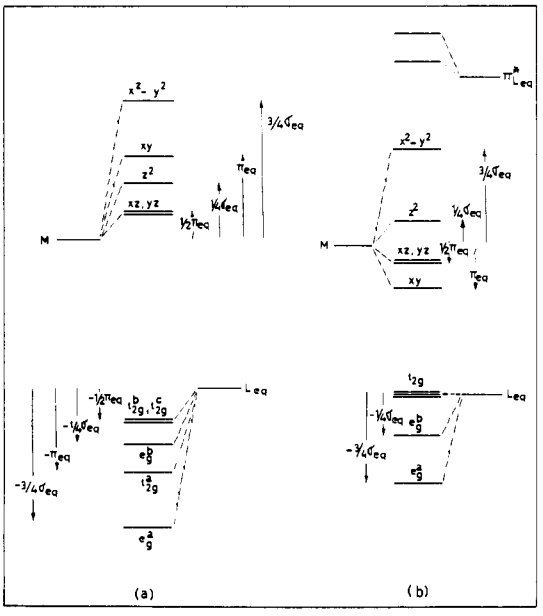


**Figure 2.** Schematic energy level diagram for the interaction of a metal $d^1$ system and one equatorial ligand in an (approximate) $D_{4h}$ environment: (a) $L_{eq}$ is a $\pi$-donor, (b) $L_{eq}$ is a $\pi$-acceptor.

it will generally be possible to select one axis (say $z$) which is quite different from the other two ($x$ and $y$). Since the off-diagonal matrix element contains $(\bar{\sigma}_x - \bar{\sigma}_y)$, it will then always be small and can be neglected in a first approximation. Therefore, even in the general case, the symmetry will at least approximately be $D_{4h}$. Replacing $\bar{\sigma}_z$ by $\bar{\sigma}_{ax}$ and $\bar{\sigma}_x \sim \bar{\sigma}_y$ by $\bar{\sigma}_{eq}$, the perturbation matrix can be expressed by means of these average axial and equatorial parameters. If so, only the diagonal elements will be nonzero: the five real d orbitals remain unaffected in all cases and are characterized by the following energies:

$$E(z^2) = 2\bar{\sigma}_{ax} + \bar{\sigma}_{eq}$$
$$E(xz) = E(yz) = 2\bar{\pi}_{ax} + 2\bar{\pi}_{eq}$$
$$E(xy) = 4\bar{\pi}_{eq}$$
$$E(x^2-y^2) = 3\bar{\sigma}_{eq} \qquad (2)$$

In eq 2, the contribution of each ligand L is additive and can be considered separately; this contribution will be different, depending on whether the ligand is in axial or equatorial position ($L_{ax}$ or $L_{eq}$). Figure 1 shows schematically the energetic effect of an axial ligand.

In Figure 1a, L is a $\pi$-bonding ligand ($\sigma_{ax} > 0$; $\pi_{ax} > 0$). In order to account for the bonding interactions as well, it is assumed that the ligand basis orbitals are stabilized to the same extent that the metal orbitals are destabilized. Thus an axial metal–ligand interaction contributes to the stabilization of the octahedral ligand group orbitals $e_g^a$ and $e_g^b$ to the extent 0 and $-\sigma$; the three $t_{2g}$ ligand group orbitals are stabilized to the extent $-\pi$, $-\pi$, and 0. If L is a $\pi$-acceptor (Figure 1b), the metal $(xz, yz)$ orbitals are taken to be stabilized by the M–L $\pi^*$-interaction ($\sigma_{ax} > 0$; $\pi_{ax} < 0$). A $\sigma$-donor can be obtained from either scheme by letting $\pi_{ax} = 0$. Figure 2 shows the corresponding diagram for the equatorial ligands.

For instance the destabilization of $d_{x^2-y^2}$, due to the four equatorial ligands is simply given by the sum of the four separate (${}^3/_4\sigma_{eq}$) parameters. It should be stressed here that the parameters for an individual ligand, $\sigma_{ax}$, $\pi_{eq}$, etc. are not to be confused with the average parameters $\bar{\sigma}_{ax}$, $\bar{\pi}_{eq}$, etc. The stabilization of each of the five (fully occupied) $e_g$- and $t_{2g}$- ligand group orbitals is assumed to be equal to the destabilization of the matching d orbital; the $e_g^a$ orbital has the same transformation properties as $d_{x^2-y^2}$, $e_g^b$ as $d_{z^2}$, etc.

The schematic representations in Figures 1 and 2 are obviously very crude. Indeed, for a $\pi$-donor, all L$\pi^*$-interactions are neglected, while for a $\pi$-acceptor, all L$\pi$-interactions were omitted. The schemes therefore represent only the net energetic effects in a qualitative way.

The bond energy $I$(M–L) for a many-electron system is defined by

$$I(\text{M-L}) = -\sum_i n_i E_i \qquad (3)$$

where the summation runs over the orbitals $i$ (bonding and antibonding); $n_i$ is the occupation number of the $i$th orbital *in the hexacoordinated complex*, and $E_i$ is the energy of the $i$th orbital *as shown in Figure 1* if L is an axial ligand *or as shown in Figure 2* if L is an equatorial ligand. The quantity $I$(M–L) cannot be expected to be an adequate approximation of the thermodynamic bond energy: an obvious and very important correction factor would include the global energy shifts of the relevant orbitals due to the change in their diagonal matrix

**Table I.** Bond Energies $I^*$(M-L) for Axial and Equatorial Ligands in the Excited Configurations of $d^3$ and $d^6$ Complexes[a]

| | | $\sigma$ or $\pi$ donor ($\pi \geq 0$) | | $\pi$ acceptor ($\pi < 0$) | |
|---|---|---|---|---|---|
| | | $z^2$ | $x^2-y^2$ | $z^2$ | $x^2-y^2$ |
| | | $d^3$ Systems ($Cr^{3+}$); Excitation $t \rightarrow e$ | | | |
| $I^*(M-L_{ax})$ | $xy$ | $\sigma_{ax} + 2\pi_{ax}$ | $2\sigma_{ax} + 2\pi_{ax}$ | $\sigma_{ax} - 2\pi_{ax}$ | $2\sigma_{ax} - 2\pi_{ax}$ |
| | $xz, yz$ | $\sigma_{ax} + 3\pi_{ax}$ | $2\sigma_{ax} + 3\pi_{ax}$ | $\sigma_{ax} - \pi_{ax}$ | $2\sigma_{ax} - \pi_{ax}$ |
| $I^*(M-L_{eq})$ | $xy$ | $\frac{7}{4}\sigma_{eq} + 3\pi_{eq}$ | $\frac{5}{4}\sigma_{eq} + 3\pi_{eq}$ | $\frac{7}{4}\sigma_{eq} - \pi_{eq}$ | $\frac{5}{4}\sigma_{eq} - \pi_{eq}$ |
| | $xz, yz$ | $\frac{7}{4}\sigma_{eq} + \frac{5}{2}\pi_{eq}$ | $\frac{5}{4}\sigma_{eq} + \frac{5}{2}\pi_{eq}$ | $\frac{7}{4}\sigma_{eq} - \frac{3}{2}\pi_{eq}$ | $\frac{5}{4}\sigma_{eq} - \frac{3}{2}\pi_{eq}$ |
| | | $d^6$ Systems ($Co^{3+}$); Excitation $t \rightarrow e$ | | | |
| $I^*(M-L_{ax})$ | $xy$ | $\sigma_{ax}$ | $2\sigma_{ax}$ | $\sigma_{ax} - 4\pi_{ax}$ | $2\sigma_{ax} - 4\pi_{ax}$ |
| | $xz, yz$ | $\sigma_{ax} + \pi_{ax}$ | $2\sigma_{ax} + \pi_{ax}$ | $\sigma_{ax} - 3\pi_{ax}$ | $2\sigma_{ax} - 3\pi_{ax}$ |
| $I^*(M-L_{eq})$ | $xy$ | $\frac{7}{4}\sigma_{eq} + \pi_{eq}$ | $\frac{5}{4}\sigma_{eq} + \pi_{eq}$ | $\frac{7}{4}\sigma_{eq} - 3\pi_{eq}$ | $\frac{5}{4}\sigma_{eq} - 3\pi_{eq}$ |
| | $xz, yz$ | $\frac{7}{4}\sigma_{eq} + \frac{1}{2}\pi_{eq}$ | $\frac{5}{4}\sigma_{eq} + \frac{1}{2}\pi_{eq}$ | $\frac{7}{4}\sigma_{eq} - \frac{7}{2}\pi_{eq}$ | $\frac{5}{4}\sigma_{eq} - \frac{7}{2}\pi_{eq}$ |

[a] The different expressions for $\pi$-donor, $\sigma$-donor, and $\pi$-acceptor ligands are listed separately. The excitation $t \rightarrow e$ can be obtained as ($xy$ or $xr,yz$) $\rightarrow$ ($z^2$ or $x^2-y^2$).

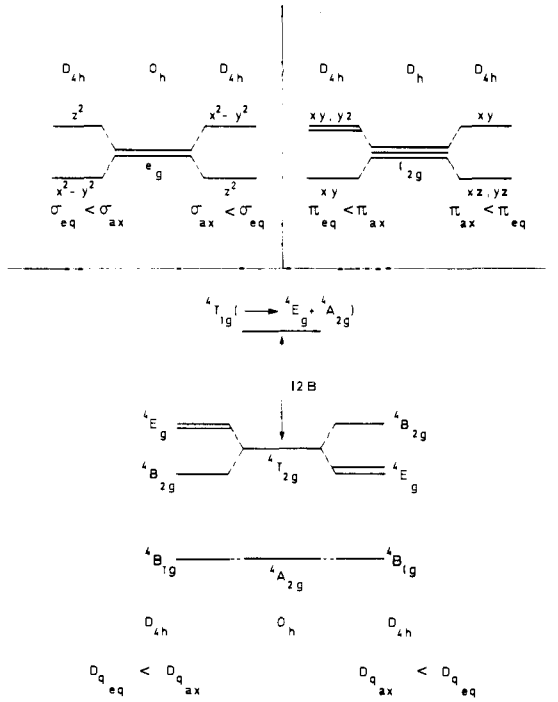


**Figure 3.** Partial orbital and state energy level diagram for hexacoordinated $d^3$ systems.

elements. $I$(M-L) includes *only* spectroscopic parameters and, as such, it can be used optimally in the study of photochemical effects. In the next sections, we consider the energy of the different M-L bonds in the excited state: $I^*$(M-L).

**Application to $d^3$ and $d^6$ Systems.** The $Cr^{3+}$ and $Co^{3+}$ octahedral complexes provide the most extensive set of experimental data, and can suitably be taken to test the methodology of the previous section. The relevant photoexcitations correspond to $t^3 \rightarrow t^2e$ and $t^6 \rightarrow t^5e$ transitions for $Cr^{3+}$ and $Co^{3+}$ complexes, respectively. In Table I, the different $I^*$(M-L) expressions are given for the possible photoactive configurations in hexacoordinated $d^3$ and $d^6$ systems.

The ground state expressions $I$(M-L) are not listed in Table I. They can easily be derived, however, and they can be shown to be identical for $L_{ax}$ and $L_{eq}$. Indeed, for example in hexacoordinated Cr(III) complexes, the ground state $t^3$ contains the five fully occupied ligand orbitals, designated $e_g^{a,b}$ and $t_{2g}^{a,b,c}$ in Figure 1a, as well as the metal subconfiguration $xy^1xz^1yz^1$. In the case of $\pi$-donor ligands, the metal holes contributing to $I$(M-$L_{ax}$) are $xy$, $xz$, and $yz$ (each once) and $z^2$, $x^2-y^2$ (each twice), yielding $I(M-L_{ax}) = 2\sigma + 2\pi$. From Figure 2a, $I(M-L_{eq}) = \pi + \frac{1}{2}\sigma + \pi + \frac{3}{2}\sigma = 2\sigma + 2\pi$. Such an isotropy would also be predicted by related bonding theories, notably by the approach of Burdett,[16] or of Hoffmann.[17]

This isotropy is not conserved in the excited states. As an example of how the entries in Table I are obtained, consider the case of $I^*(M-L_{eq})$ in Co(III) surrounded by six $\pi$-acceptor ligands. One of the excited configurations corresponds to the $xy \rightarrow z^2$ excitation. The five ligand orbitals $e_g$ and $t_{2g}$ are again fully occupied, while the ligand $\pi^*$-orbitals are empty. Figure 2b shows that the $\sigma$-interactions contribute to $I^*$ through the metal holes $(z^2)^1$ and $(x^2-y^2)^2$, i.e., $\frac{1}{4}\sigma + 2(\frac{3}{4}\sigma) = \frac{7}{4}\sigma$; for the $\pi$-interactions, the contribution comes from the metal electrons $xy^1xz^2yz^2$, i.e., $4(-\frac{1}{2}\pi) + 1(-\pi) = -3\pi$.

Certain obvious regularities are apparent from the expressions in Table I. For instance it is interesting to compare $I^*(M-L)_{eq}$ and $I^*(M-L)_{ax}$ for a specific configuration and a given ligand. The population of $d_{z^2}$ destabilizes the axial ligand with respect to the equatorial ligand to the amount of $\frac{3}{4}\sigma$; population of $d_{x^2-y^2}$ has exactly the opposite effect. Depopulation of $d_{xy}$ does not affect the M-$L_{ax}$ bond but it modifies the M-$L_{eq}$ bond strength by $\pi$ energy units (stabilization for $\pi$-donor and destabilization for $\pi$-acceptor ligands). The opposite holds true for depopulation of the ($d_{xz}$, $d_{yz}$) orbitals, where the net difference between $I^*(M-L_{eq})$ and $I^*(M-L_{ax})$ amounts to $-(\pi/2)$ energy units.

In order to determine the dominant $D_{4h}$ configuration in the photoexcited states, electron repulsion effects have to be taken into account. Figure 3 shows a partial state energy level diagram for $Cr^{3+}$ complexes, as compared to the orbital energy level diagrams.

Both $^4T_{2g}$ and $^4T_{1g}$ correspond to the $O_h$ $t^2e$ configuration; they are separated by $12B$. The strong field wave functions are given by[18]

$$\begin{aligned}
^4B_{2g}&: |(xz)(yz)(x^2-y^2)| \\
^4E_g(^4T_{2g})&: |(xz)(xy)[\sqrt{3}/2(z^2) - \tfrac{1}{2}(x^2-y^2)]| \\
&\quad\ |(yz)(xy)[\sqrt{3}/2(z^2) - \tfrac{1}{2}(x^2-y^2)]| \\
^4A_{2g}&: |(xz)(yz)(z^2)| \\
^4E_g(^4T_{1g})&: |(xz)(xy)[-\tfrac{1}{2}(z^2) - \sqrt{3}/2(x^2-y^2)]| \\
&\quad\ |(yz)(xy)[-\tfrac{1}{2}(z^2) - \sqrt{3}/2(x^2-y^2)]| \quad (4)
\end{aligned}$$

The first-order energy splittings caused by the tetragonal field, are

$$\begin{aligned}
E(^4B_{2g}) - E(^4E_g;\ ^4T_{2g}) &= 2(\bar{\pi}_{ax} - \bar{\pi}_{eq}) - \tfrac{3}{2}(\bar{\sigma}_{ax} - \bar{\sigma}_{eq}) \\
&= \tfrac{1}{2}(10\overline{Dq}_{eq} - 10\overline{Dq}_{ax}) \quad (5)
\end{aligned}$$

**Table II.** Spectrochemical $\sigma$ and $\pi$-Parameters for a Number of $Cr^{3+}$-L Interactions[a]

| Ligand | $\sigma_L'$ | $\pi_L'$ | $10Dq$ | Ref |
|---|---|---|---|---|
| $I^-$ | −2600 | 650 | 11 150 | 21 |
| $Br^-$ | −2100 | 850 | 11 850 | 19-21 |
| $Cl^-$ | −1600 | 900 | 13 150 | 19-21 |
| $H_2O$ | −1240 | 500 | 15 830 | 19, 22 |
| $F^-$ | 450 | 1700 | 16 100 | 19-21 |
| $NCS^-$ | −770 | 380 | 17 720 | 19 |
| $OH^-$ | 940 | 1390 | 18 810 | 20 |
| $NH_3$; en | 0 | 0 | 21 550 | 23 |
| $CN^-$ | 1300 | −290 | 26 610 | 23 |

[a] All values are expressed with respect to the $NH_3$ case: $\sigma_L' = \sigma_L - \sigma_{NH_3}$; $\pi_L' = \pi_L - \pi_{NH_3}$ and as usual $\pi_{NH_3} \simeq 0$.

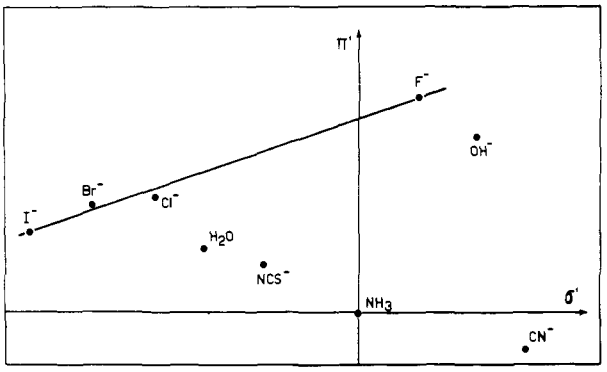


**Figure 4.** Two-dimensional spectrochemical series for a number of common ligands in hexacoordinated Cr(III) complexes.

$$E(^4A_{2g}) - E(^4E_g; {}^4T_{1g}) = 2(\bar{\pi}_{ax} - \bar{\pi}_{eq}) + \tfrac{3}{2}(\bar{\sigma}_{ax} - \bar{\sigma}_{eq}) \quad (6)$$

where $10Dq = 3\sigma - 4\pi$.

As has been pointed out by Zink,[7] the situation will be modified in second order due to the interaction between the two $^4E_g$ states. If the tetragonal perturbation is represented by $\mathcal{V}_4$, one finds

$$\Psi(^4E_g; {}^4T_{2g})|\mathcal{V}_4|\Psi(^4E_g; {}^4T_{1g}) = \frac{\sqrt{3}}{2}(\bar{\sigma}_{eq} - \bar{\sigma}_{ax}) \quad (7)$$

and a mixing coefficient

$$c = \frac{\sqrt{3}(\bar{\sigma}_{ax} - \bar{\sigma}_{eq})}{24B} \quad (8)$$

The $d_{z^2}$ character $x$ in $^4E_g(^4T_{2g})$ is then

$$x = \frac{1}{1 + c^2}\left[\frac{\sqrt{3} - c}{2}\right]^2 \quad (9)$$

For $c = 0$ (octahedral case), this expression of course reduces to $\frac{3}{4}$. The $d_{z^2}$-content increases if $\bar{\sigma}_{eq} > \bar{\sigma}_{ax}$, it decreases if $\bar{\sigma}_{ax} > \bar{\sigma}_{eq}$; this conclusion is independent of the relative value of the $\pi$ parameters. The same line of reasoning leads to similar expressions for the $E_g$ states of the $Co^{3+}$-$d_6$ complexes.

**Comparison with Experiment.** Since the $I^*$(M-L) values of Table I are expressed in terms of the spectrochemical $\sigma$ and $\pi$ parameters, a comparison of the present model with the photochemical data requires the numerical value of these parameters. In Table II, a number of important M-L parameters are listed for $Cr^{3+}$ complexes. Figure 4 shows the corresponding two-dimensional spectrochemical series.

In the subsequent calculation of the spectrochemical parameters, the $Co^{3+}$ parameters were taken to be the same as the $Cr^{3+}$ parameters; from a comparison of the relevant $10Dq$ values, this approximation does not seem to be unreasonable.[24]

The most important photochemical data are listed in Table III, where the experimentally observed dominant reaction mode is given for each complex.

The "leaving ligand" (predicted) is considered to be the ligand with the lowest value of $I^*$(M-L). In general, $I^*$(M-L) is evaluated as follows: (i) the lowest excited ligand field state is determined from eq 5. If $10\overline{Dq}_{ax} < 10\overline{Dq}_{eq}$, $^4E_g$ is the photoactive state of the $d^3$ system; if $10\overline{Dq}_{ax} > 10\overline{Dq}_{eq}$, the photoactive state is $^4B_{2g}$. Here, of course

$$10\overline{Dq}_{ax} = 3\bar{\sigma}_{ax} - 4\bar{\pi}_{ax} = \tfrac{3}{2}(\sigma_z + \sigma_{-z}) - 2(\pi_z + \pi_{-z})$$

$$10\overline{Dq}_{eq} = 3\bar{\sigma}_{eq} - 4\bar{\pi}_{eq} = \tfrac{3}{4}(\sigma_x + \sigma_{-x} + \sigma_y + \sigma_{-y}) - (\pi_x + \pi_{-x} + \pi_y + \pi_{-y})$$

If $d^6$ complexes are considered, the photoactive states are $^3E_g$ and $^3A_{2g}$, respectively. (ii) The relevant state functions are given by eq 4, modified where necessary by the interaction described in eq 7 and 8. In this way, one obtains the contribution of the different excited configurations to the photoactive state. (iii) For each excited configuration and for each ligand, $I^*$(M-L) can now be found from Table I. As an example, consider *trans*-$[Cr(NH_3)_4(NCS)Cl]^+$

$$\overline{Dq}_{ax} = \tfrac{1}{2}[Dq(NCS) + Dq(Cl)]$$

$$\overline{Dq}_{eq} = Dq(NH_3)$$

Since $\overline{Dq}_{ax} < \overline{Dq}_{eq}$, the photoactive state is considered to be $^4E_g(^4T_{2g})$

$$\bar{\sigma}_{ax} = \tfrac{1}{2}[\sigma(NCS) + \sigma(Cl)]$$

$$\bar{\sigma}_{eq} = \sigma(NH_3)$$

Using the numerical values of Table II, and letting $B = 700$ $cm^{-1}$ for $Cr^{3+}$ (600 $cm^{-1}$ for $Co^{3+}$), the composition of the $^4E_g$ state is found to be approximately 84.6% $(xz, yz)^1(xy)^1(z^2)^1$ and 15.4% $(xz, yz)^1(xy)^1(x^2 - y^2)^1$. Therefore

$$I^*(Cr\text{-}NCS) = 0.846[\sigma(NCS) + 3\pi(NCS)] + 0.154[2\sigma(NCS) + 3\pi(NCS)]$$

$$I^*(Cr\text{-}Cl) = 0.846[\sigma(Cl) + 3\pi(Cl)] + 0.154[2\sigma(Cl) + 3\pi(Cl)]$$

$$I^*(Cr\text{-}NH_3) = [(0.846)(7/4) + (0.154)(5/4)]\sigma(NH_3)$$

While comparing theory and experiment, no attempt was made to explain the absolute values of the different quantum yields. Indeed, the study of reaction rates is intimately coupled with the study of the competing photophysical processes. For the same reason, the data are restricted to irradiation in the lowest energy component of the first ligand field absorption band. Photosubstitution, which shows involvement of mechanisms due to secondary effects, such as redox mechanisms or excited-state base hydrolysis are outside the realm of this model.

Possible stereochemical modifications in the course of the reaction are assumed not to interfere with the initial dissociation of the irradiated complex. The present model is focused exclusively on the latter process; the stereochemistry of the substitution reactions will be considered in a separate paper.

## Discussion of the Results

With the above restrictions in mind, Table III exhibits a quasi-perfect agreement between theory and experiment: the leaving ligand is correctly predicted in all cases.

**(A) Comparison with Adamson's Rules.** In order to analyze the results of Table III, it is useful to consider the excitation process as the distribution of the photon energy over the different (M-L) sites of the complex. In order to do so, one has

**Table III**

| Complex | $I^*$(M-L) values (in $cm^{-1}$) | | | | $x$ | Leaving L (predicted) | Leaving L (dominant reaction mode obsd) | Ref |
|---|---|---|---|---|---|---|---|---|
| $[Cr(NH_3)_5X]^{n+}$ | $I^*(M\text{-}X_{ax})$ | $I^*(M\text{-}NH_3)_{ax}$ | $I^*(M\text{-}NH_3)_{eq}$ | | | | | |
| $Cr(NH_3)_5NCS^{2+}$ | 8 950 | 8 740 | 11 790 | | 0.783 | $(NH_3)_{ax}$ | $(NH_3)_{ax}$ | 25 |
| $Cr(NH_3)_5Cl^{2+}$ | 9 300 | 8 500 | 11 910 | | 0.817 | $(NH_3)_{ax}$ | $(NH_3)_{ax}$ | 25 |
| $Cr(NH_3)_5Br^{2+}$ | 8 465 | 8 360 | 11 980 | | 0.836 | $(NH_3)_{ax}$ | $(NH_3)_{ax}$ | 25 |
| $Cr(NH_3)_5H_2O^{3+}$ | 8 610 | 8 600 | 11 860 | | 0.803 | $(NH_3)_{ax}$, $H_2O$ | $NH_3$ | 25, *a* |
| *trans*-$[Cr(Z)_4X_2]^{n+}$, ... $XY]^{n+}$ | $I^*(M\text{-}X_{ax}$ | $I^*(M\text{-}Y)_{ax}$ | $I^*(M\text{-}Z)_{eq}$ | | | | | |
| *trans*-$Cr(NH_3)_4(H_2O)_2^{3+}$ | 8 330 | | 12 030 | | 0.85 | $(H_2O)$ | $(H_2O)$ | 25 |
| *trans*-$Cr(NH_3)_4(NCS)Cl^{+}$ | 8 540 | 9 140 | 12 010 | | 0.846 | $NCS^-$ | $NCS^- > Cl^-$ | 25 |
| *trans*-$Cr(NH_3)_4(H_2O)Cl^{2+}$ | 8 260 | 9 050 | 12 080 | | 0.863 | $H_2O$ | $H_2O$ | 25 |
| *trans*-$Cr(NH_3)_4(H_2O)NCS^{2+}$ | 8 435 | 8 620 | 11 970 | | 0.833 | $H_2O$ | $H_2O$ | 25 |
| *trans*-$Cr(NCS)_4(NH_3)_2^-$ | 14 360 | | 9 150 | | | $NCS^-$ | $NCS^-$ | 26 |
| *trans*-$Cr(en)_2Cl_2^+$ | 8 980 | | 12 120 | | 0.875 | $Cl^-$ | $Cl^-$ | 39 |
| *trans*-$Cr(en)_2ClF^+$ | 9 400 | 14 260 | 11 850 | | 0.80 | $Cl^-$ | $Cl^-$ | 27 |
| *trans*-$Cr(en)_2(NCS)_2^+$ | 8 740 | | 11 900 | | 0.815 | $NCS^-$ | $NCS^- > en$ | 28 |
| *trans*-$Cr(en)_2F_2^+$ | 14 960 | | 11 520 | | 0.708 | en | en | 29 |
| *trans*-$Cr(en)_2(NCS)Cl^+$ | 8 540 | 9 140 | 12 010 | | 0.846 | $NCS^-$ | $NCS^- > Cl^-$ | 30 |
| *cis*-$[Cr(en)_2XY]^{n+}$ | $I^*(M\text{-}X_{eq})$ | $I^*(M\text{-}Y_{eq})$ | $I^*(M\text{-}en_{eq})$ | $I^*(M\text{-}en_{ax})$ | | | | |
| *cis*-$Cr(en)_2(NCS)Cl^+$ | 9 155 | 9 680 | 8 980 | 14 370 | | $(en)_{eq}$ | en | 30 |
| *cis*-$Cr(en)_2Cl_2^+$ | 9 680 | | 8 980 | 14 370 | | $(en)_{eq}$ | en | 39 |
| $[Co(Z)_5X]^{n+}$ | $I^*(M\text{-}X_{ax})$ | $I^*(M\text{-}Z_{ax})$ | $I^*(M\text{-}Z_{eq})$ | | | | | |
| $Co(CN)_5NH_3^{2-}$ | 8 150 | 10 490 | 15 290 | | 0.866 | $NH_3$ | $NH_3$ | 2 |
| $Co(CN)_5Cl^{3-}$ | 6 880 | 9 950 | 15 560 | | 0.93 | $Cl^-$ | $Cl^-$ | 2 |
| $Co(CN)_5Br^{3-}$ | 6 190 | 9 780 | 15 650 | | 0.95 | $Br^-$ | $Br^-$ | 2 |
| $Co(CN)_5I^{3-}$ | 5 390 | 9 640 | 15 710 | | 0.966 | $I^-$ | $I^-$ | 2 |
| $Co(CN)_5H_2O^{2-}$ | 7 950 | 10 075 | 15 500 | | 0.915 | $H_2O$ | $H_2O$ | 31 |
| $Co(CN)_5OH^{3-}$ | 11 325 | 11 240 | 14 880 | | 0.77 | $(CN^-)_{ax}$ | $CN^-$ | 32 |
| $Co(NH_3)_5Cl^{2+}$ | 7 265 | 8 180 | 12 060 | | 0.86 | $Cl^-$ | $Cl^-$, $NH_3$ | 2, *b* |
| $Co(NH_3)_5Br^{2+}$ | 6 490 | 7 973 | 12 175 | | 0.89 | $Br^-$ | $Br^-$ | 35 |
| $Co(NH_3)_5NCS^{2+}$ | 8 040 | 8 570 | 11 870 | | 0.806 | $NCS^-$ | $NCS^-$ | 2 |
| *trans*-$[Co(Z)_4XY]^{n+}$ | $I^*(M\text{-}X_{ax})$ | $I^*(M\text{-}Y_{ax})$ | $I^*(M\text{-}Z_{eq})$ | | | | | |
| *trans*-$Co(CN)_4(OH)_2^{3-}$ | 11 105 | | 15 030 | | 0.804 | $OH^-$ | $OH^-$ | 33 |
| *trans*-$Co(en)_2(NCS)Cl^+$ | 7 400 | 7 015 | 12 230 | | 0.905 | $Cl^-$ | $NCS^- \approx Cl^-$ | 36 |
| *cis*-$[Co(Z)_4X_2]^{n+}$ | $I^*(M\text{-}X_{eq})$ | $I^*(M\text{-}Z_{eq})$ | $I^*(M\text{-}Z_{ax})$ | | | | | |
| *cis*-$Co(CN)_4(OH)_2^{3-}$ | 11 545 | 11 470 | 18 125 | | | $(CN^-)_{eq}$ | $CN^-$ | 33 |
| *cis*-$Co(en)_2Cl_2^+$ | 7 880 | 8 980 | 14 360 | | | $Cl^-$ | $Cl^-$ | 2 |

[a] For $Cr(NH_3)_5H_2O^{3+}$: photorelease of $H_2O$ was not investigated. The model predicts practically equal quantum yields for $H_2O$ as for $NH_{3\,ax}$. [b] Dominant aquation of $NH_3$ was reported upon irradiation in the highest component of the first LF absorption band, suggesting equatorial labilization (ref 34). Upon irradiation in the triplet region, however, $Cl^-$ is preferentially exchanged, in agreement with axial labilization (ref 40).

to compare the quantity $(I - I^*)$ for the different metal-ligand bonds.

If the photoactive state corresponds to an $xy \rightarrow x^2 - y^2$ excitation, the excitation energy is distributed over the equatorial bonds *only*. The equatorial metal-ligand bond weakening is simply proportional to the spectrochemical strength of the interaction: for each individual ligand one can write

$$I(M\text{-}L_{eq}) - I^*(M\text{-}L_{eq}) = \tfrac{1}{4}(3\sigma_{eq} - 4\pi_{eq}) = \tfrac{5}{2}Dq_{eq} \quad (10)$$

The axial metal-ligand bonds remain unaffected by the excitation:

$$I(M\text{-}L_{ax}) - I^*(M\text{-}L_{ax}) = 0 \quad (11)$$

When the photoactive state is $E_g$, the state functions (eq 4) are modified to some extent by configurational mixing. If this mixing is neglected as a first approximation ($x = \frac{3}{4}$ in eq 9), the $(I - I^*)$ parameter is again a simple function of the spectrochemical strength ($10Dq$) of each ligand.

$$I(M\text{-}L_{eq}) - I^*(M\text{-}L_{eq}) = \tfrac{1}{8}(3\sigma_{eq} - 4\pi_{eq}) = \tfrac{5}{4}Dq_{eq} \quad (12)$$

$$I(M\text{-}L_{ax}) - I^*(M\text{-}L_{ax}) = \tfrac{1}{4}(3\sigma_{ax} - 4\pi_{ax}) = \tfrac{5}{2}Dq_{ax} \quad (13)$$

Thus for a given $10Dq$ value, an axial bond absorbs twice as much excitation energy as an equatorial bond. These conclusions are valid for $\pi$-acceptor as well as $\pi$-donor ligands.

If the interactions between the two $E_g$ states are accounted for, $x$ becomes generally larger than $\frac{3}{4}$ (since in nearly all cases $\sigma_{ax} < \sigma_{eq}$), thereby increasing $(I - I^*)_{ax}$ and decreasing $(I - I^*)_{eq}$. Thus, introduction of configurational mixing will weaken the axial bonds even more and the equatorial bonds even less than could be expected from eq 12 and 13.

If $(I - I^*)$ were the determining parameter in the photosubstitution process, the previous considerations would lead us directly to Adamson's rules. Indeed, the average ligand field, $\overline{Dq}_{ax}$ or $\overline{Dq}_{eq}$, determines the photoactive state. If $\overline{Dq}_{ax} > \overline{Dq}_{eq}$, the photoactive state corresponds predominantly to the $(xy \rightarrow x^2 - y^2)$ excitation, and according to eq 10 and 11, only the equatorial ligands are labilized. If $\overline{Dq}_{ax} < \overline{Dq}_{eq}$, the photoactive state corresponds predominantly to the $(xz, yz) \rightarrow z^2$ excitation and the axial ligands are labilized at least twice as much as the equatorial ligands. This is precisely the behavior described by Adamson's first rule. In each case, eq 10 and 13

predict a labilization which is directly proportional to the $10Dq$ value of the individual ligand; this is equivalent with the second rule.

If on the other hand, the relevant parameter is not $(I - I^*)$, but $I^*$, the predictions of Table III are valid. The first and most obvious test case is *trans*-$[Cr(en)_2F_2]^+$, where Adamson's first rule predicts axial labilization, whereas from Table III, one expects an equatorial release. Indeed, the $(xz, yz \rightarrow z^2)$ excitation does destabilize the Cr-F axis more than the Cr-N axis. However, the ground state bond energy $I(Cr\text{-}F) = 2\sigma(F) + 2\pi(F)$ is much larger than $I(Cr\text{-}N)$, due to the strong $\sigma$- and $\pi$-donor properties of fluorine; the net balance yields $I^*(Cr\text{-}F) > I^*(Cr\text{-}N)$, which explains the experimentally observed release of ethylenediamine. This conclusion is reinforced by configuration interaction, $x$ being less than $\frac{3}{4}$ in this particular case.

In all other cases under consideration, the predictions of Adamson's *first* rule and the methodology of Table III are identical.

**(B) The Leaving Ligand.** The difference between the two models becomes more apparent when one considers the leaving ligand on the labilized axis.

(1) If $\overline{Dq}_{ax} < \overline{Dq}_{eq}$, the photoactive $^4E_g$ state of the Cr(III) complexes is characterized by

$$I^*(M\text{-}L_{ax}) = (2 - x)\sigma_{ax} + 3\pi_{ax} \quad (14)$$

$$I^*(M\text{-}L_{eq}) = \tfrac{1}{4}(5 + 2x)\sigma_{eq} + \tfrac{5}{2}\pi_{eq} \quad (15)$$

where $x$ is the fraction of $d_{z^2}$ character (eq 9). For equatorial labilization, eq 15 cannot really be put to test, since the only corresponding complex, *trans*-$Cr(en)_2F_2^+$, has four identical equatorial ligands.

In the case of axial labilization, eq 14 shows that the relevant quantity to be evaluated for the two ligands is $(2 - x)\sigma_{ax} + 3\pi_{ax}$. Application of this formalism predicts correctly the leaving ligand for all the experimental data of Table III.

In a few cases, the $I^*(M\text{-}L)$ values for both ligands are quite close to each other, and only application of configuration interaction leads to the correct answer. From eq 9, it follows that $x > \frac{3}{4}$ for $\bar{\sigma}_{ax} < \bar{\sigma}_{eq}$. Assuming that the Racah parameter $B \simeq 700\ cm^{-1}$, the $Cr(NH_3)_5Br^{2+}$ complex is characterized by $x = 0.836$ and the $Cr(NH_3)_5H_2O^{3+}$ complex by $x = 0.803$.

It should be pointed out that the predictions from the two models are different for *trans*-$[Cr(en)_2FCl]^+$ and *trans*-$[Cr(NH_3)_4(H_2O)(NCS)]^{2+}$. It is experimentally verified that in both complexes the ligand with the *smallest* spectrochemical strength is released preferentially. It is true that the Cr-F and the Cr-NCS bonds absorb more excitation energy than the Cr-Cl and Cr-$H_2O$ bonds, respectively. However, the ground state bond energy $I(M\text{-}L)$ is in both cases decisively larger for the strongest field ligand.

As for the substituted Co(III)-ammines and -cyanides, axial labilization is predicted in all cases where $\overline{Dq}_{ax} < \overline{Dq}_{eq}$. $I^*(M\text{-}L_{ax})$ is given by an expression similar to eq 14, but where the factor multiplying $\pi_{ax}$ is not 3, but 1. Table III shows a very good agreement between predicted and observed leaving ligands.

Adamson's second rule predicts exchange of the transamine in both $Cr(NH_3)_5X^{2+}$ and $Co(NH_3)_5X^{2+}$. Experimentally, this is found to be true for Cr(III), but not for Co(III), exactly as expected from the previous considerations. Indeed, in the Co(III) complexes—as opposed to Cr(III)—the $\pi$-donor properties of the X ligand provide no net contribution to the ground state energy $I(Co\text{-}X)$. Therefore, the stability difference between the MX and M-$NH_3$ bonds is considerably larger in Co(III) than in Cr(III) compounds.

The $Co(CN)_5X$ complexes would be expected to release the trans cyano group if Adamson's second rule is followed. In fact, except when $X = OH^-$, the X group is released. Indeed, Table III shows that the relevant quantity $(2 - x)\sigma + \pi$ is larger for $OH^-$ than $I^*(Co\text{-}CN^-)$, mainly due to the strong $\pi$-donor properties of $OH^-$, while for all other $X^-$ ligands, the weaker $\sigma$-donor properties of X are the dominant factor making the Co-X bond weaker than Co-CN.

(2) If $\overline{Dq}_{ax} > \overline{Dq}_{eq}$, the equatorial photolabilization is due to $(xy \rightarrow x^2 - y^2)$ excitation. The only examples available are *cis*-$Cr(en)_2Cl_2^+$, *cis*-$Cr(en)_2(NCS)Cl^+$, *cis*-$Co(en)_2Cl_2^+$, and *cis*-$Co(CN)_4(OH)_2^{3-}$. The relevant expressions are

$$I^*(M\text{-}L_{eq}) = \tfrac{5}{4}\sigma_{eq} + y\pi_{eq} \quad (16)$$

where $y = 3$ for the Cr(III) and 1 for the Co(III) complexes. The smallest $I^*$ values are found for Cr-en, Co-Cl, and Co-CN, respectively; these predictions are again confirmed by the experimental data. It should be noted that Adamson's second rule would predict the wrong result for *cis*-$[Co(en)_2Cl_2]^+$.

## Conclusions

The methodology based on the evaluation of $I^*(M\text{-}L)$ is presented as an alternative to Adamson's rules. The fact that *all* the experimental data of Table III are reproduced correctly is certainly coincidental to some extent. It is almost certain that sooner or later exceptions will be found. Moreover, the uncertainty on the value of the spectroscopic $\sigma$ and $\pi$ parameters alone might cast some doubt on any "perfect" agreement between theory and experiment.

We believe, however, that the present method provides an adequate description of the observed phenomena in terms of a limited set of relevant parameters. The factors multiplying $\sigma$ and $\pi$ in Table I and in the different equations do not have immediate quantitative meaning. They should rather be considered as a rough measure of the weight of a particular bonding type in the ground and excited states; they might be compared to some extent to the bond orders in the theory of diatomic molecules.

Extension of the model to the photochemistry of heavier transition metals[37] and metal carbonyls[38] is seriously handicapped by the lack of reliable parameters.

## References and Notes


(1) V. Balzani and V. Carasitti, "Photochemistry of Coordination Compounds", Academic Press, London, 1970.
(2) A. W. Adamson and P. D. Fleischauer Ed., "Concepts of Inorganic Photochemistry", Wiley Interscience, New York, N.Y., 1975.
(3) A. W. Adamson, *J. Phys. Chem.*, 71, 798 (1967).
(4) J. I. Zink, *J. Am. Chem. Soc.*, **94**, 8039 (1972).
(5) J. I. Zink, *Inorg. Chem.*, **12**, 1018 (1973).
(6) J. I. Zink, *Mol. Photochem.*, **5**, 151 (1973).
(7) J. I. Zink, *Inorg. Chem.*, **12**, 1957 (1973).
(8) J. I. Zink, *J. Am. Chem. Soc.*, **96**, 4464 (1974).
(9) M. J. Incorvia and J. I. Zink, *Inorg. Chem.*, **13**, 2489 (1974).
(10) M. Wrighton, H. B. Gray, and G. S. Hammond, *Mol. Photochem.*, **5**, 164 (1973).
(11) C. Furlani, *Theor. Chim. Acta*, **34**, 233 (1974).
(12) D. S. McClure, "Advances in the Chemistry of Coordination Compounds, Proceedings of the Sixth International Conference on Coordination Chemistry", Macmillan, New York, N.Y., 1961, p 498.
(13) C. E. Schäffer, "XIIth International Conference on Coordination Chemistry Sydney 1969", IUPAC London, Butterworths, 1970, p 361.
(14) L. G. Vanquickenborne, J. Vranckx, and C. Görller-Walrand, *J. Am. Chem. Soc.*, **96**, 4121 (1974).
(15) C. K. Jørgensen, "Modern Aspects of Ligand Field Theory", Elsevier, 1971, p 178.
(16) J. K. Burdett, *Inorg. Chem.*, **15**, 212 (1976).
(17) M. Elian and R. Hoffmann, *Inorg. Chem.*, **14**, 1058 (1975).
(18) J. R. Perumareddi, *J. Phys. Chem.*, **71**, 3144 (1967).
(19) W. W. Fee and J. N. MacB. Harrowfield, *Aust. J. Chem.*, **23**, 1049 (1970).
(20) M. Keeton, B. Fa-Chun Chou, and A. B. P. Lever, *Can. J. Chem.*, **49**, 192 (1972).
(21) J. Glerup, O. Mønsted, and C. E. Schäffer, *Inorg. Chem.*, **15**, 1399 (1976).
(22) Parameters for $H_2O$ are particularly uncertain. The values used demonstrate the weak $\pi$-donor character of $H_2O$.
(23) J. R. Perumareddi, *Coord. Chem. Rev.*, **4**, 73 (1969).
(24) C. K. Jørgensen, *Struct. Bonding (Berlin)*, **1** (1966).
(25) A. D. Kirk, *Mol. Photochem.*, **5**, 127 (1973), and references therein.
(26) E. E. Wegner and A. W. Adamson, *J. Am. Chem. Soc.*, **88**, 394 (1966).
(27) G. Wirth and R. G. Linck, *J. Am. Chem. Soc.*, **95**, 5913 (1973).
(28) C. Bifano and R. G. Linck, *Inorg. Chem.*, **13**, 609 (1974).

(29) S. G. Pyke and R. G. Linck, *J. Am. Chem. Soc.*, **93**, 5281 (1971).
(30) M. T. Gandolfi, M. F. Manfrin, A. Juris, L. Moggi, and V. Balzani, *Inorg. Chem.*, **13**, 1342 (1974).
(31) M. Wrighton and D. Bredesen, *Inorg. Chem.*, **12**, 1707 (1973).
(32) L. Viaene, J. D'Olieslager, and S. De Jaegere, *Bull. Soc. Chim. Belg.*, **83**, 31 (1974).
(33) L. Viaene, Doctoral Thesis, Louvain 1975.
(34) R. A. Pribush, C. K. Poon, C. M. Bruce, and A. W. Adamson, *J. Am. Chem. Soc.*, **96**, 3027 (1974).
(35) H. Gafney and A. W. Adamson, *Coord. Chem. Rev.*, **16**, 171 (1975).
(36) P. S. Sheridan and A. W. Adamson, *J. Am. Chem. Soc.*, **96**, 3032 (1974).
(37) P. C. Ford, J. D. Petersen, and R. E. Hintze, *Coord. Chem. Rev.*, **14**, 67 (1974).
(38) M. Wrighton, *Chem. Rev.*, **74**, 401 (1974).
(39) A. D. Kirk, K. C. Moss, and J. G. Valentin, *Can. J. Chem.*, **49**, 1524 (1971).
(40) C. H. Langford and C. P. J. Vuik, *J. Am. Chem. Soc.*, **98**, 5409 (1976).

# Kinetics of the Electron-Transfer Reactions of Azaviolene Radical Ions. 2.[1] Correlation with the Marcus Theory. The Question of Concerted Acid–Base Catalysis

**Claude F. Bernasconi* and Hsien-chang Wang**

*Contribution from the Thimann Laboratories of the University of California, Santa Cruz, California 95064.* *Received August 31, 1976*

**Abstract:** The comproportionation–disproportionation kinetics of the azaviolene redox systems derived from 1-ethyl-2-quinolone azine (I), 1-ethyl-2-pyridone azine (III), and 1,3-dimethyl-2-benzimidazolone azine (IV) have been studied in 50% acetonitrile–50% water (v/v), IV also in 50% 2-methoxyethanol–50% water (v/v), by temperature-jump, stopped-flow, and pH-jump techniques. Electron transfer was found to occur by three concurrent pathways, viz., (1) Red + $Ox^{2+} \rightleftarrows Sem^+ + Sem^+$, (2) $RedH^+ + Ox^{2+} \rightleftarrows Sem^+ + SemH^{2+}$, and (3) a concerted general acid–base catalyzed reaction $RedH^+ + Ox^{2+} + B^- \rightleftarrows Sem^+ + Sem^+ + BH$; Red is the reduced, $Ox^{2+}$ the oxidized, and $Sem^+$ is the semireduced form of the redox system. The kinetics of the cross reactions, $_1Red + {}_2Ox^{2+} \rightleftarrows {}_1Sem^+ + {}_2Sem^+$, have also been measured for the pairs I(Red) + III($Ox^{2+}$) and II($Red^{2-}$) + III($Ox^{2+}$) where II is 1-ethyl-2-quinolone-6-sulfonate azine. The rate and equilibrium constants correlate very well with the Marcus theory. The observation and/or absence, respectively, of concerted general acid–base catalysis is discussed by using More O'Ferral's and Jencks' method of estimating the free-energy surface of the system based on the free energies of the four corners of the contour map. Concerted catalysis is observed when the free energies of the two unstable intermediates are similar and high compared with the reactants and/or when the activation barrier for the electron transfer is very low which leads to enforced concerted catalysis.

Azaviolenes are a class of compounds which can exist in three different oxidation states, with the general structures shown.[2] Electron transfer from one state of another can occur

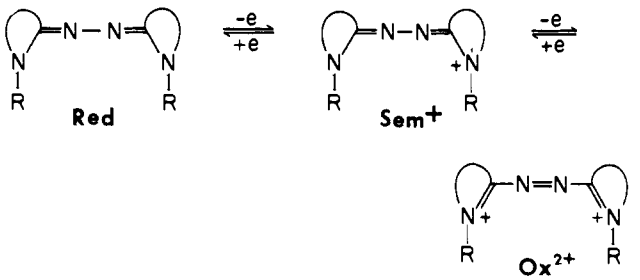


by the comproportionation–disproportionation reaction 1.

$$\text{Red} + Ox^{2+} \underset{k_{-1}}{\overset{k_1}{\rightleftharpoons}} 2Sem^+ \qquad (1)$$

In the first part of this series[1] we reported a kinetic study of the comproportionation–disproportionation of the systems derived from 1-ethyl-2-quinolone azine (I) and 1-ethyl-2-quinolone-6-sulfonate azine (II) in 50% 2-methoxyethanol–50% water (v/v) (ME–$H_2O$). Owing to the protonation of Red[3] on the bridge nitrogens,[4] to form $RedH^+$ [3] and $RedH_2^{2+}$,[3] two additional electron-transfer pathways had to be considered as shown in Scheme I. The rate law showed that for I all three pathways are significant, whereas for II only the two pathways $k_1$–$k_{-1}$ and $k_2$–$k_{-2}$ were detectable. Furthermore, the rate was found to be dependent on buffer concentration, suggesting a general acid–base catalyzed pathway:

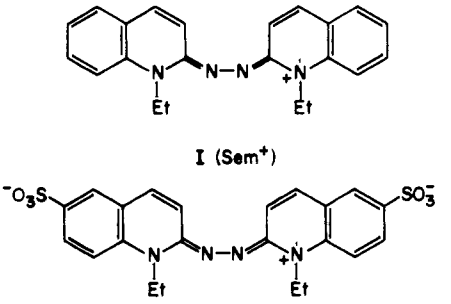


Scheme I

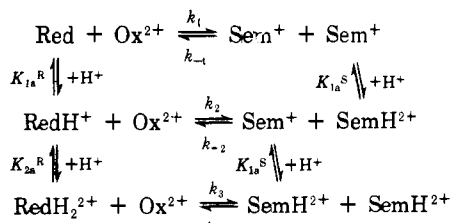


$$RedH^+ + Ox^{2+} + B^- \underset{k_{-2}^{BH}}{\overset{k_2^B}{\rightleftharpoons}} Sem^+ + Sem^+ + BH \qquad (2)$$

We have now extended this work to the systems derived from 1-ethyl-2-pyridone azine (III) and 1,3-dimethyl-2-benzimidazolone azine (IV), and also by measuring the cross reactions